The effect of extratropical cyclones on satellite-retrieved aerosol properties over ocean

B. S. Grandey,[1] P. Stier,[1] T. M. Wagner,[1] R. G. Grainger,[1] and K. I. Hodges[2]

Received 8 April 2011; revised 25 May 2011; accepted 26 May 2011; published 8 July 2011.

[1] Extratropical cyclones may have a significant effect on column aerosol properties over ocean. European Centre for Medium Range Weather Forecasts (ECMWF) derived storm-centric composites of Moderate Resolution Imaging Spectroradiometer (MODIS) and Advanced Along-Track Scanning Radiometer (AATSR) aerosol optical depth and aerosol size parameters are produced for the North Atlantic and the South Atlantic oceans. It is found that retrieved aerosol optical depth and aerosol size both increase near the center of the composite extratropical cyclones. Using composites of ECMWF ERA-Interim reanalysis data, it is demonstrated that wind speed is a considerably more likely explanatory variable than relative humidity for the aerosol observations. A comparison of composites for both MODIS and AATSR, which uses a wind speed dependent sea-surface brightness model in the aerosol retrieval, suggests that although surface brightness effects may contribute towards some of the observations, wind speed dependent emission of sea salt also appears to make a significant contribution to the observed aerosol properties. **Citation:** Grandey, B. S., P. Stier, T. M. Wagner, R. G. Grainger, and K. I. Hodges (2011), The effect of extratropical cyclones on satellite-retrieved aerosol properties over ocean, *Geophys. Res. Lett.*, *38*, L13805, doi:10.1029/2011GL047703.

1. Introduction

[2] Meteorological effects may lead to spurious correlations between aerosol and cloud properties [e.g., *Stevens and Feingold*, 2009]. It is therefore important to understand the effect synoptic systems may have on cloud and aerosol properties.

[3] Over land, synoptic conditions often appear to be a major factor affecting aerosol air pollution [*Dharshana et al.*, 2010]. Cold fronts have been observed to remove aerosols near the surface [e.g., *Sheih et al.*, 1983; *Jia et al.*, 2008].

[4] Over ocean, high wind speeds and relative humidities associated with synoptic storms can lead to significantly increased aerosol optical depth [*Glantz et al.*, 2009], due to both hygroscopic growth of aerosols [e.g., *Seinfeld and Pandis*, 1998] and increased sea salt emission [e.g., *Woodcock*, 1953; *Lewis and Schwartz*, 2004]. Above a certain wind speed threshold, it is possible that sea salt concentrations near the surface may decrease due to scavenging by spray droplets [*Pant et al.*, 2008]. However, the question remains as to how extratropical cyclones may affect total column aerosol properties.

[5] Previous compositing studies have looked at the dynamical structure of extratropical cyclones [e.g., *Catto et al.*, 2010] and the effect that extratropical cyclones have on clouds over ocean [*Lau and Crane*, 1995, 1997; *Norris and Iacobellis*, 2005; *Wang and Rogers*, 2001; *Chang and Song*, 2006; *Field and Wood*, 2007; *Field et al.*, 2008]. This study seeks to complement these previous studies through the production of storm-centric composites of satellite-retrieved total column aerosol properties over ocean.

[6] In this study, the following question is asked: What effect do extratropical cyclones have on column aerosol properties over ocean?

2. Method

[7] This study uses satellite-retrieved aerosol properties over ocean from both the Moderate Resolution Imaging Spectroradiometer (MODIS) on Aqua and the Advanced Along-Track Scanning Radiometer (AATSR) on ENVISAT. Aerosol optical depth at 550 nm (τ) and fine-mode fraction data from the MODIS Science Team Collection 5 Atmosphere Level 2 Joint Product are used [*Remer et al.*, 2005]. The MODIS aerosol data are provided at approximately 10 km × 10 km resolution. No wind speed dependent sea-surface brightness correction is applied in the Collection 5 aerosol retrieval.

[8] In order to allow comparison with an independent aerosol dataset which has a wind speed dependent sea-surface brightness correction, AATSR τ and Ångström exponent data retrieved by the Oxford-RAL Retrieval of Aerosols and Clouds (ORAC) as part of the GlobAEROSOL project are also used [*Thomas et al.*, 2009; *Sayer et al.*, 2010]. Each GlobAEROSOL daily file provides data on a 10 km × 10 km sinusoidal grid. The accuracy of both of these retrieval algorithms is discussed by *Kokhanovsky et al.* [2010].

[9] Relative vorticity at 850 hPa, zonal and meridional components of the 10-metre wind, mean sea level pressure (p_0) and 850 hPa relative humidity (RH) are provided in European Centre for Medium Range Weather Forecasts (ECMWF) ERA-Interim reanalysis data. The reanalysis data used here are at 6 hourly temporal and 1.5° × 1.5° spatial resolution. Wind speed (u) is calculated using the 10-metre wind vector components.

[10] Extratropical cyclones are tracked using TRACK [*Hodges*, 1995, 1999]. TRACK has been configured to track 850 hPa relative vorticity associated with extratropical cyclones, henceforth referred to as storms. Storms which persist for less than two days or move a distance of less than 1000 km are not considered.

[11] For each storm at each model time-step, p_0, RH and the wind data are regridded at 200 km × 200 km resolution

[1]Atmospheric, Oceanic and Planetary Physics, Department of Physics, University of Oxford, Oxford, UK.
[2]Environmental Systems Science Centre, University of Reading, Reading, UK.

0094-8276/11/2011GL047703

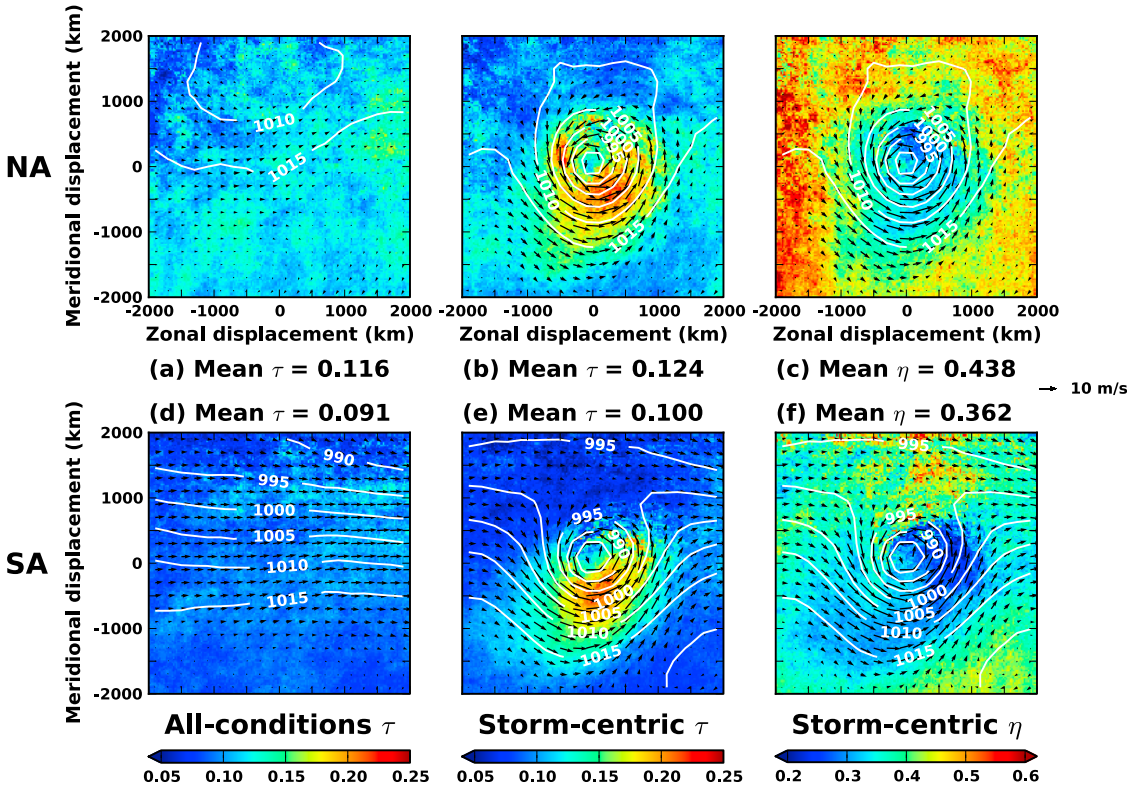

Figure 1. Aqua-MODIS (a and d) all-conditions aerosol optical depth (τ), (b and e) storm-centric τ, and (c and f) storm-centric fine-mode fraction (η) median composites for the North Atlantic (NA; Figures 1a–1c) and the South Atlantic (SA; Figures 1d–1f) oceans. Composite ERA-Interim mean sea level pressure (p_0; white contours) and wind vectors (black arrows) are overplotted. The wind vector scale is provided at the right-hand edge. Positive meridional displacements are poleward of the storm center.

on a 4000 km × 4000 km domain centered on the storm. In order to produce storm-centric satellite-retrieved aerosol data, the tracked cyclone locations and relative vorticities are interpolated to five minute temporal resolution, using a parametric cubic spline with time as the parameter. If Aqua-MODIS or AATSR retrieved aerosol data exist within a 4000 km × 4000 km storm-centric domain, then the aerosol data are regridded at 25 km × 25 km resolution on the storm-centric domain.

[12] The storm-centric regularly gridded model and satellite data for individual storms are then composited. The advantages of looking at a composite storm are that data coverage of the storm-centric domain will be increased significantly, that noise will be reduced and that background variability will be largely removed, making some statistically relevant large-scale structure more evident than in individual cases. In order to reduce the unrepresentative influence of extreme aerosol events, the composites are produced using medians.

[13] In order to compare against average conditions, the reanalysis and satellite data are also regridded with respect to storm tracks which have been translated temporally by one year. This allows for the production of all-conditions composites from data which are blind as to whether or not a storm is present in the domain but which also have the same seasonal and locational sampling as the storm-centric composites.

[14] Composites for storms over the North Atlantic ocean (NA; 50°W–10°W, 30°N–55°N) and South Atlantic ocean (SA; 50°W–10°E, 55°S–30°S) are compared. A minimum 850 hPa relative vorticity threshold of 7×10^{-5} s^{-1} has been chosen, leading to median storm-center p_0 values of 988 hPa and 980 hPa for the NA and the SA respectively. Throughout this study, 5 years (2003–2007) of data, covering all seasons, are used.

3. Results and Discussion

[15] Figures 1a and 1d show all-conditions MODIS τ composites for the NA and the SA. Although some noise is evident, these composite fields are relatively smooth and no large-scale structure is evident. It can be seen that the NA generally experiences higher τ than the SA, most likely due to anthropogenic aerosol pollution advected from North America.

[16] Storm-centric τ composites are shown in Figures 1b and 1e. Towards the edge of the domains, τ is similar to that of the corresponding all-conditions composites, with higher τ for the NA than the SA. However, towards the center of the domain it can be seen that storms can have a strong effect on τ compared to average conditions. For both the NA and the SA, τ increases near the center of the storm-centric composites, peaking equatorward of the low pressure center.

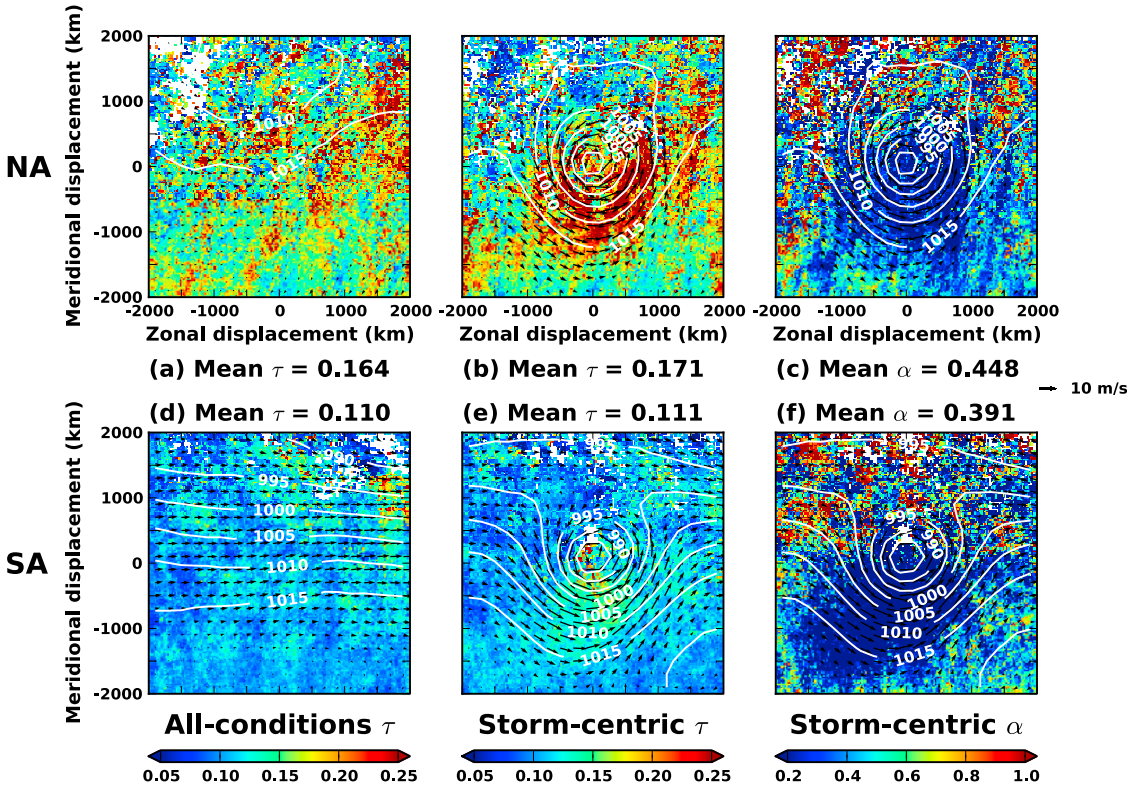

Figure 2. Same as Figure 1, but for GlobAEROSOL AATSR (a and d) all-conditions aerosol optical depth (τ), (b and e) storm-centric τ, and (c and f) storm-centric Ångström exponent (α) composites. White fill represents missing data.

[17] In order to provide an indication of the size distribution of the observed aerosol, storm-centric MODIS fine-mode fraction is shown in Figures 1c and 1f. Near the edge of the storm domain it can be seen that fine-mode fraction is higher for the NA than the SA, consistent with there being more anthropogenic fine-mode aerosol in the NA. In the regions of higher u near the center of the composites, where the enhanced τ was also observed, fine-mode fraction is smaller, indicating the presence of larger aerosols.

[18] Two physical mechanisms may explain the increase in τ and decrease in fine-mode fraction towards the center of the composite storms. First, increasing u will result in increased sea-salt emission [*Lewis and Schwartz*, 2004]. Sea-salt aerosol is often large, so this would result in a decrease in fine-mode fraction alongside an increase in τ, as observed. Second, *RH* (not shown) is higher nearer the center of the storm, leading to hygroscopic growth of aerosol particles [*Seinfeld and Pandis*, 1998]. This too would result in a decrease in fine-mode fraction as well as an increase in τ.

[19] In addition to the two physical mechanisms mentioned above, it is possible that the results observed in Figure 1 may be due to a retrieval error. Increasing u leads to a brightening of the ocean surface. This would lead to an increase in retrieved τ and may also affect fine-mode fraction. This sea-surface brightness effect is not corrected for in the MODIS Collection 5 aerosol data. It is also worth noting that some of the aerosol retrievals may be contaminated by cloud such as thin cirrus [e.g., *Huang et al.*, 2011], although this would not explain the storm-centric τ and fine-mode fraction patterns shown in Figure 1.

[20] In order to investigate the possible contribution of a surface brightness retrieval error to these observations, Figure 2 shows similar composites for GlobAEROSOL AATSR data. The GlobAEROSOL AATSR retrieval has a wind speed dependent sea-surface brightness correction, although some residual sea-surface brightness contamination may remain. This retrieval is independent of the MODIS retrieval.

[21] As can be seen in Figure 2, the AATSR composites provide incomplete coverage and are significantly noisier than the MODIS composites shown in Figure 1. This is due to AATSR having a smaller swath width than MODIS. The presence of missing data in the poleward part of the AATSR composites is due to there being fewer AATSR retrievals at high latitudes compared to lower latitudes.

[22] However, despite the noise, the AATSR composites have a similar structure to the MODIS composites. The all-conditions τ is higher in the NA than in the SA. The GlobAEROSOL AATSR often amplifies high τ, resulting in higher τ observations in the NA compared to the MODIS τ observations. AATSR τ is generally higher in regions of higher u towards the center of the storm domains compared to regions of lower u. Figures 2c and 2f show storm-centric composites of Ångström exponent, which is inversely related to aerosol size. It can be seen that aerosol size increases towards the center of the composite storms, as was also observed in the MODIS composites.

[23] Both the MODIS and AATSR datasets indicate an increase in τ near the center of the composite storms. The fact that these observations apply to two independent satellite datasets, one of which has a wind speed dependent sea-surface brightness correction, suggests that surface brightness effects cannot fully account for these observations.

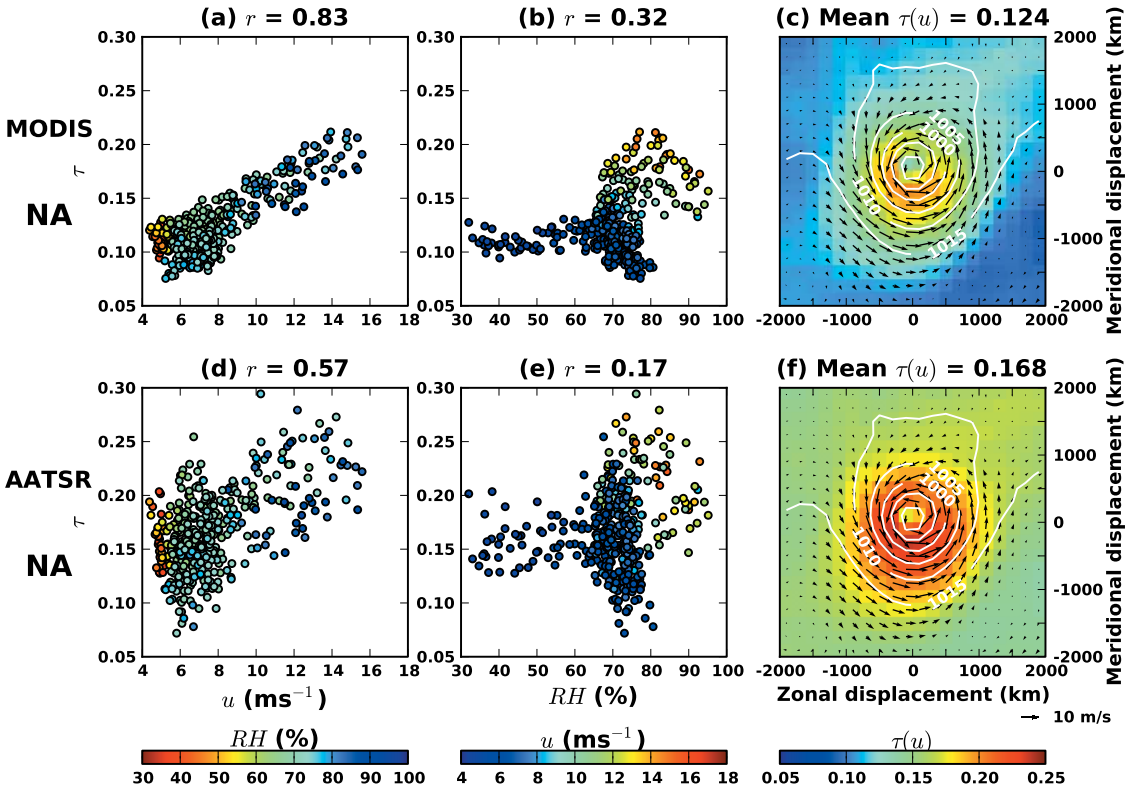

Figure 3. (a) Scatter plot of North Atlantic (NA) storm-centric composited Aqua-MODIS aerosol optical depth (τ) against wind speed (u) colored according to relative humidity (RH). Each point in the scatter plot corresponds to a 200 km × 200 km grid point in Figure 1b. (b) A similar scatter plot for τ against RH, colored according to u. (c) u-fitted linear model predicted $\tau(u)$ based on the coefficients in the first row of Table 1: $\tau(u) = 0.0496 + 0.0097u$. (d–f) Similar to Figures 3a–3c, but for NA AATSR τ. Similar scatter plots and u linear model predictions for the other MODIS and AATSR aerosol properties for both the NA and the South Atlantic (SA) can be viewed in the auxiliary material.

Therefore, one or both of the physical mechanisms of sea salt emission and hygroscopic growth must be a major contributor to these observations.

[24] As mentioned above, both RH and u generally increase towards the center of the storm domain. Storm-centric composite RH (not shown) generally peaks very close to the center of the storm domain, being negatively correlated to p_0, with p_0–RH pattern correlation coefficients [*Glickman*, 2000] of $r = -0.75$ and $r = -0.93$ for the NA and the SA respectively. Storm-centric composite u is also correlated to p_0, with p_0–u $r = -0.76$ and $r = -0.41$ for the NA and the SA respectively, but u peaks equatorward of the storm center. As can be seen in Figures 1 and 2, storm-centric τ also peaks equatorward of the storm center, with a similar spatial pattern to the winds. Visual comparison of τ and the wind fields of the storm-centric composites in Figures 1 and 2 suggests that u is the dominant explanatory variable for τ.

[25] This is investigated further by looking at u–τ and RH–τ pattern correlations. Storm-centric τ is regridded to the 200 km × 200 km resolution of the u and RH fields. Figure 3a shows an example scatter plot of NA storm-centric MODIS τ against u (see also auxiliary material).[1] As can be seen, there is an approximately linear relationship between u and τ, with a good pattern correlation ($r = 0.83$). A linear relationship between u and τ is consistent with the findings of *Smirnov et al.* [2003] and other studies referenced by them. By comparison, the scatter plot of NA storm-centric MODIS τ against RH (Figure 3b) shows a much weaker and less linear relationship between RH and τ ($r = 0.32$). This supports the argument that u is the primary explanatory variable for NA storm-centric MODIS τ. The u–RH pattern correlation ($r = 0.62$) is stronger than the RH–τ correlation, suggesting that non-orthoganality between u and RH may be driving the RH–τ correlation. Interestingly, for fixed u, looking along a vertical line in Figure 3a or a fixed color in Figure 3b, there often appears to be a negative RH–τ correlation, opposite to that which would be expected for the conceptual aerosol hygroscopic growth model.

[26] A linear regression model, of form $\tau(u) = a + bu$, has been fitted to the NA storm-centric τ data shown in Figure 3a. The resulting coefficients are shown in the first row of Table 1. This model has then be used to make a prediction of τ using u as the only input field. The resulting NA storm-centric $\tau(u)$ is shown in Figure 3c. By visual inspection of Figures 1b and 3c, it can be clearly seen that a linear regression model based only on u is capable of reproducing the significant features of NA storm-centric MODIS τ.

[27] For comparison, Figures 3d–3f show corresponding scatter plots and predicted $\tau(u)$ for NA storm-centric AATSR τ. It can be seen that a linear relationship between u and τ is less clear here than it is for the MODIS data.

[1] Auxiliary materials are available in the HTML. doi:10.1029/2011GL047703.

Table 1. Linear Regression Slopes (b), Intercepts (a), and Pattern Correlation Coefficients (r) of Aerosol Properties (Aerosol Optical Depth τ, Fine-Mode Fraction η, and Ångström Exponent α) Against Wind Speed (u) Across the North Atlantic (NA) and South Atlantic (SA) Storm-Centric Composite Domains[a]

	u			
	b (m^{-1} s)	a	r	RH r
NA MODIS τ	0.0097 ± 0.0003	0.0496	0.83	0.32
SA MODIS τ	0.0111 ± 0.0004	0.0041	0.83	0.22
NA AATSR τ	0.0089 ± 0.0006	0.0997	0.57	0.17
SA AATSR τ	0.0034 ± 0.0003	0.0813	0.54	0.19
NA MODIS η	−0.0184 ± 0.0007	0.5793	−0.80	−0.38
SA MODIS η	−0.0115 ± 0.0007	0.4621	−0.61	−0.21
NA AATSR α	−0.0388 ± 0.0033	0.7575	−0.51	−0.05
SA AATSR α	−0.0461 ± 0.0038	0.8030	−0.52	0.04

[a]The final column contains r for aerosol properties against relative humidity (RH). The pattern correlation coefficients between u and RH are 0.62 and 0.54 for the NA and the SA respectively.

A lower pattern correlation is found, probably due to a combination of increased noise in the AATSR data and surface brightness effects in the MODIS data. However, as with the MODIS data, it can be seen that u is a more appropriate explanatory variable than RH.

[28] The first four rows in Table 1 contain u–τ and RH–τ pattern correlation coefficients, as well as u linear regression model coefficients, for the different MODIS/AATSR and NA/SA combinations. The r values show that τ is always more strongly correlated to u than to RH.

[29] For both MODIS and AATSR separately, the intercept (a) is lower in the NA than in the SA, consistent with higher background pollution in the NA. The slopes (b) for NA MODIS, SA MODIS and NA AATSR $\tau(u)$ are comparable. However, b is much lower for SA AATSR $\tau(u)$. The reason for the higher MODIS and NA AATSR b may be that MODIS overestimates the u–τ relationship due to surface brightness effects and AATSR amplifies high τ. The values of a and b calculated here for SA storm-centric composite AATSR τ ($a = 0.0813$, $b = 0.0034 \pm 0.0003$) are similar to those previously found for the remote southern ocean by *Huang et al.* [2010] ($a = 0.0850 \pm 0.0002$, $b = 0.0040 \pm 0.0002$) who used temporally and spatially matched τ and u data in their analysis.

[30] The final four rows of Table 1 show pattern correlation coefficients and u linear regression model coefficients for the aerosol size parameters. These also show strong relationships with u, although the linear models for the size parameters do not work quite as well as for the $\tau(u)$ models.

4. Conclusions

[31] As demonstrated, midlatitude synoptic storm systems have a significant effect on storm-centric composite aerosol properties, with retrieved aerosol optical depth and aerosol size increasing substantially in regions of high wind speed near the center of extratropical cyclones over ocean. By producing composites of both MODIS Collection 5 aerosol data, which have no wind speed dependent sea-surface brightness correction, and GlobAerosol AATSR aerosol data, which do have a wind speed dependent sea-surface brightness correction, it has been shown that sea-surface brightness effects alone cannot account for the observed storm-centric aerosol signals. Pattern correlations and linear regression models, applied across the storm-centric composite domains, have shown that wind speed is a suitable explanatory variable for the aerosol properties. The results are consistent with wind speed dependent emission of sea-salt.

[32] Midlatitude storms are also a major driver of cloud properties [*Field and Wood*, 2007]. The extent to which extratropical cyclones may be responsible for driving satellite-observed relationships between midlatitude aerosol and cloud properties will be explored in future work.

[33] **Acknowledgments.** MODIS data were obtained from the Level 1 and Atmosphere Archive and Distribution System (LAADS). The ERA-Interim Reanalysis data were provided by ECMWF. This work was supported by a UK Natural Environment Research Council (NERC) DPhil studentship and also the NERC AEROS project (NE/G006148/1). TMW acknowledges support from the John Fell Fund. RGG acknowledges support from the NERC National Centre for Earth Observation.

[34] The Editor thanks William Cotton and an anonymous reviewer for their assistance in evaluating this paper.

References

Catto, J. L., L. C. Shaffrey, and K. I. Hodges (2010), Can climate models capture the structure of extratropical cyclones?, *J. Clim.*, *23*, 1621–163, doi:10.1175/2009JCLI3318.1.

Chang, E. K. M., and S. Song (2006), The seasonal cycles in the distribution and precipitation around cyclones in the western North Pacific and Atlantic, *J. Atmos. Sci.*, *63*, 815–839.

Dharshana, K. G. T., S. Kravtsov, and J. D. W. Kahl (2010), Relationship between synoptic weather disturbances and particulate matter air pollution over the United States, *J. Geophys. Res.*, *115*, D24219, doi:10.1029/2010JD014852.

Field, P. R., and R. Wood (2007), Precipitation and cloud structure in midlatitude cyclones, *J. Clim.*, *20*(2), 233–254, doi:10.1175/JCLI3998.1.

Field, P. R., A. Gettelman, R. B. Neale, R. Wood, P. J. Rasch, and H. Morrison (2008), Midlatitude cyclone compositing to constrain climate model behaviour using satellite observations, *J. Clim.*, *21*, 5887–5903, doi:10.1175/2008JCLI2235.1.

Glantz, P., E. D. Nilsson, and W. von Hoyningen-Huene (2009), Estimating a relationship between aerosol optical thickness and surface wind speed over the ocean, *Atmos. Res.*, *92*, 58–68, doi:10.1016/j.atmosres.2008.08.010.

Glickman, T. (Ed.) (2000), *Glossary of Meteorology*, 2nd ed., Am. Meteorol. Soc., Boston, Mass.

Hodges, K. I. (1995), Feature tracking on the unit sphere, *Mon. Weather Rev.*, *123*, 3458–3465.

Hodges, K. I. (1999), Adaptive constraints for feature tracking, *Mon. Weather Rev.*, *127*, 1362–1373.

Huang, H., G. E. Thomas, and R. G. Grainger (2010), Relationship between wind speed and aerosol optical depth over remote ocean, *Atmos. Chem. Phys.*, *10*(13), 5943–5950, doi:10.5194/acp-10-5943-2010.

Huang, J., N. C. Hsu, S.-C. Tsay, M.-J. Jeong, B. N. Holben, T. A. Berkoff, and E. J. Welton (2011), Susceptibility of aerosol optical thickness retrievals to thin cirrus contamination during the BASE-ASIA campaign, *J. Geophys. Res.*, *116*, D08214, doi:10.1029/2010JD014910.

Jia, Y., K. A. Rahn, K. He, T. Wen, and Y. Wang (2008), A novel technique for quanifying the regional component of urban aerosol solely from its sawtooth cycles, *J. Geophys. Res.*, *113*, D21309, doi:10.1029/2008JD010389.

Kokhanovsky, A. A., et al. (2010), The inter-comparison of major satellite aerosol retrieval algorithms using simulated intensity and polarization characteristics of reflected light, *Atmos. Meas. Tech.*, *3*(4), 909–932, doi:10.5194/amt-3-909-2010.

Lau, N.-C., and M. W. Crane (1995), A satellite view of the synoptic-scale organization of cloud properties in midlatitude and tropical circulation systems, *Mon. Weather Rev.*, *123*, 1984–2006.

Lau, N.-C., and M. W. Crane (1997), Comparing satellite and surface observations of cloud patterns in synoptic-scale circulation systems, *Mon. Weather Rev.*, *125*, 3172–3189.

Lewis, E. R., and S. E. Schwartz (Eds.) (2004), *Sea Salt Aerosol Production: Mechanisms, Methods, Measurements, and Models*, *Geophys. Monogr. Ser.*, vol. 152, AGU, Washington, D. C.

Norris, J. R., and S. F. Iacobellis (2005), North Pacific cloud feedbacks inferred from synoptic-scale dynamic and thermodynamic relationships, *J. Clim.*, *18*, 4862–4878.

Pant, V., C. G. Deshpande, and A. K. Kamra (2008), On the aerosol number concentration–wind speed relationship during a severe cyclonic

storm over south Indian Ocean, *J. Geophys. Res.*, *113*, D02206, doi:10.1029/2006JD008035.

Remer, L. A., et al. (2005), The MODIS aerosol algorithm, products, and validation, *J. Atmos. Sci.*, *62*(4), 947–973, doi:10.1175/JAS3385.1.

Sayer, A. M., G. E. Thomas, and R. G. Grainger (2010), A sea surface reflectance model for (A)ATSR, and application to aerosol retrievals, *Atmos. Meas. Tech.*, *3*(4), 813–838, doi:10.5194/amt-3-813-2010.

Seinfeld, J. H., and S. N. Pandis (1998), *Atmospheric Chemistry and Physics: From Air Pollution to Climate Change*, John Wiley, New York.

Sheih, C. M., S. A. Johnson, and F. T. DePaul (1983), Case studies of aerosol size distribution and chemistry during passages of a cold and a warm front, *Atmos. Environ.*, *17*(7), 1299–1306, doi:10.1016/0004-6981(83)90404-3.

Smirnov, A., B. N. Holben, T. F. Eck, O. Dubovik, and I. Slutsker (2003), Effect of wind speed on columnar aerosol optical properties at Midway Island, *J. Geophys. Res.*, *108*(D24), 4802, doi:10.1029/2003JD003879.

Stevens, B., and G. Feingold (2009), Untangling aerosol effects on clouds and precipitation in a buffered system, *Nature*, *461*, 607–613, doi:10.1038/nature08281.

Thomas, G. E., E. Carboni, A. M. Sayer, C. A. Poulson, R. Siddans, and R. G. Grainger (2009), Oxford-RAL Aerosol and Cloud (ORAC): Aerosol retrievals from satellite radiometers, in *Satellite Aerosol Remote Sensing Over Land*, edited by A. A. Kokhanovsky and G. de Leeuw, pp. 193–225, Springer, Berlin.

Wang, C.-C., and J. C. Rogers (2001), A composite study of explosive cyclogenesis in different sectors of the North Atlantic. Part I: Cyclone structure and evolution, *Mon. Weather Rev.*, *129*, 1481–1499.

Woodcock, A. H. (1953), Salt nuclei in marine air as a function of altitude and wind force, *J. Meteorol.*, *10*(5), 362–371.

R. G. Grainger, B. S. Grandey, P. Stier, and T. M. Wagner, Atmospheric, Oceanic and Planetary Physics, Clarendon Laboratory, University of Oxford, Parks Road, Oxford OX1 3PU, UK. (grandey@atm.ox.ac.uk)

K. I. Hodges, Environmental Systems Science Centre, University of Reading, Harry Pitt Building, 3 EarleyGate, Whiteknights, PO Box 238, Reading RG6 6AL, UK.